

# Weak gravitational lensing and the Euclid space mission

Martin Kilbinger

CEA Saclay, Irfu/DAP - AIM, CosmoStat; IAP

École polytechnique, enseignement d'approfondissement  
8 novembre 2022

`martin.kilbinger@cea.fr`

`www.cosmostat.org/kilbinger`

Slides: `http://www.cosmostat.org/people/kilbinger`



`@energie_sombre`



**COSMOSTAT**



**université  
PARIS-SACLAY**



# Overview

Basics of gravitational lensing

Weak lensing measurement

Euclid

Results from current surveys

# Books, Reviews and Lecture Notes

- Kochanek, Schneider & Wambsganss 2004, book (Saas Fee) **Gravitational lensing: Strong, weak & micro**. Download Part I (Introduction) and Part III (Weak lensing) from my homepage <http://www.cosmostat.org/people/kilbinger>.
- Kilbinger 2015, review **Cosmology from cosmic shear observations** Reports on Progress in Physics, 78, 086901, arXiv:1411.0155
- Mandelbaum 2018, review **Weak lensing for precision cosmology**, ARAA submitted, arXiv:1710.03235
- Sarah Bridle 2014, lecture videos (Saas Fee) <http://archiveweb.epfl.ch/saasfee2014.epfl.ch/page-110036-en.html>

# Gravitational lensing

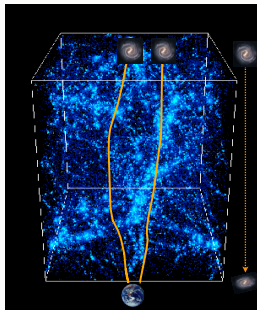
Gravitational lensing = light deflection and focusing by matter

Light is deflected by both **dark** and **luminous** matter.

Important to study dark matter:

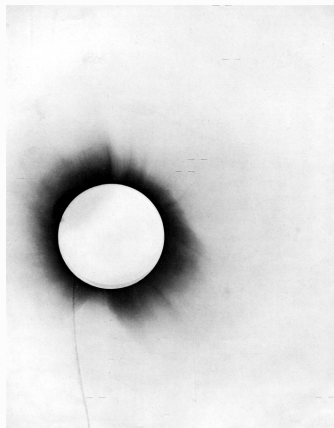
- Dominant over luminous (baryonic) matter (27% vs. 5%)
- Dark matter easy to understand and simulate ( $N$ -body simulations), only interaction is gravity

We will be looking at the small distortion of distant galaxies by the cosmic web (weak cosmological lensing, cosmic shear).



## Brief history of gravitational lensing

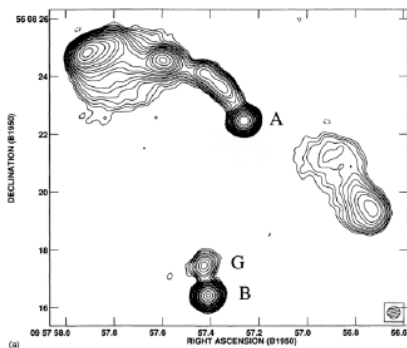
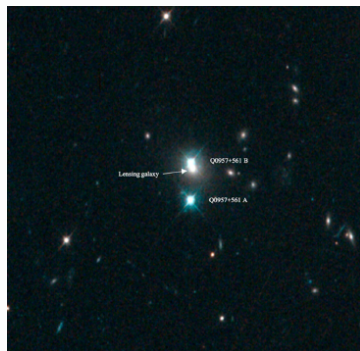
- Before Einstein: Masses deflect photons, treated as point masses.
- 1915 Einstein's GR predicted deflection of stars by sun, deflection larger by 2 compared to classical value. Confirmed 1919 by Eddington and others during solar eclipse.



Photograph taken by Eddington of solar corona, and stars marked with bars.

## Lensing on cosmological scales

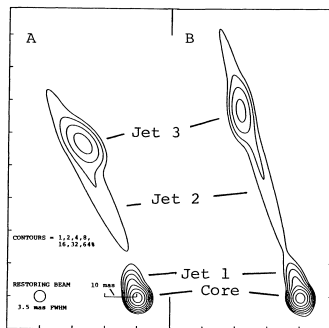
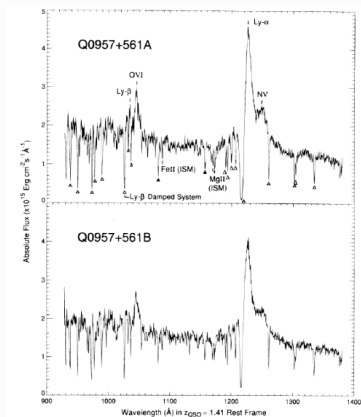
- 1979 Walsh et al. detect first double image of a lenses quasar.



(Walsh et al. 1979)

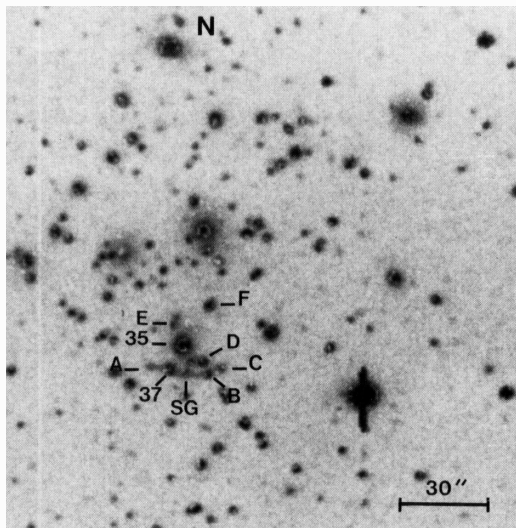
## Lensing on cosmological scales

- 1979 Walsh et al. detect first double image of a lenses quasar.



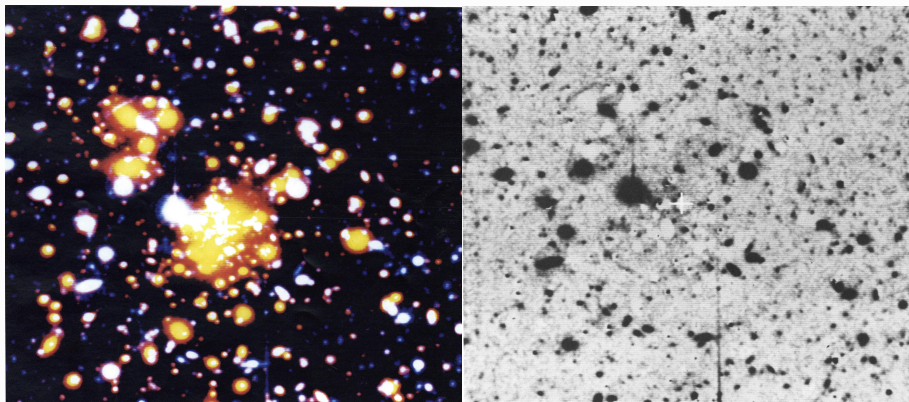
(Walsh et al. 1979)

- 1987 Soucail et al. strongly distorted “arcs” of background galaxies behind galaxy cluster, using CCDs.



exclude that it is an off-chance superimposition of faint cluster galaxies even if a diffuse component seems quite clear from the R CCD field. A gravitational lens effect on a background quasar is a possibility owing to the curvature of the structure but in fact it is too small (Hammer 86) and no blue object opposite the central galaxy has been detected. It is more likely that we are dealing with a star formation region located in the very rich core where

- Tyson et al. (1990), tangential alignment around clusters.



Abell 1689

Cluster outskirts: Weak gravitational lensing.

- 2000 **cosmic shear**: weak lensing in blind fields, by 4 groups (Edinburgh, Hawai'i, Paris, Bell Labs/US).  
Some 10,000 galaxies on an area of a few square degrees on the sky.
- 2010 - 2020s: Many dedicated surveys: DLS, CFHTLenS, DES, KiDS, HSC. Competitive constraints on cosmology.  
Factor 100 increase: Millions of galaxies over 100s of degrees. Many other improvements: Multi-band observations, photometric redshifts, image and  $N$ -body simulations, ....
- 2025 -: LSST@VRO, Roman space mission (WFIRST), Euclid data will be available.  
Another factor of 100 increase: Hundred millions of galaxies, tens of thousands of degrees area (most of the extragalactic sky).

# Light deflection

Simplest case: point mass deflects light

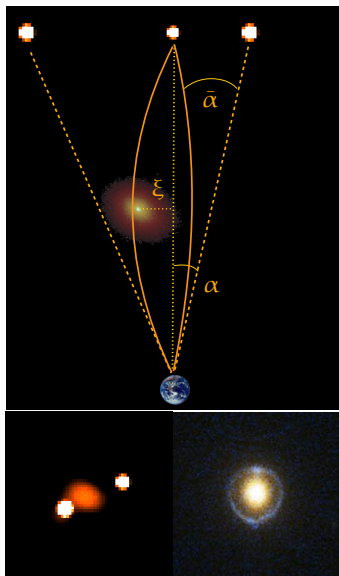
Deflection angle for a point mass  $M$  is

$$\hat{\alpha} = \frac{4GM}{c^2\xi} = \frac{2R_S}{\xi}$$

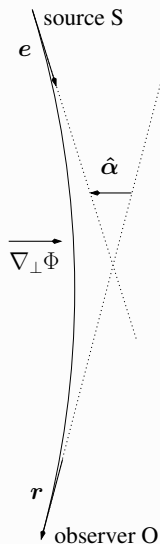
$R_S$  is the Schwarzschild radius.

(Einstein 1915)

This is twice the value one would get in a classical, Newtonian calculation.



## Deflection angle: general case



Deflection angle  $\hat{\alpha} = r - e$ .

Derive from Fermat's principle of least light travel time.

Perturbed Minkowski metric, weak-field ( $\phi \ll c^2$ )

$$ds^2 = (1 + 2\phi/c^2) c^2 dt^2 - (1 - 2\phi/c^2) dl^2$$

Light travels on geodesics,  $ds^2 = 0$

→ light travel time  $t$  is

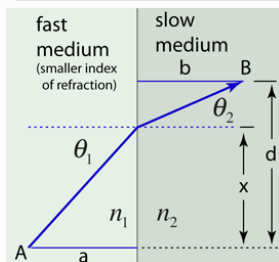
$$t = \frac{1}{c} \int_{\text{path}} (1 - 2\phi/c^2) dl$$

## Deflection angle: general case

Fermat's principle: Minimize light travel time.

Analogous to refraction in medium with refractive index  $n > 1$ ,

$$t = \frac{1}{c} \int_{\text{path}} (1 - 2\phi/c^2) dl = \frac{1}{c} \int_{\text{path}} n(\mathbf{x}) dl$$



Minimize  $t$  to derive Snell's law,  $\sin \theta_1 / \sin \theta_2 = n_2 / n_1$ .

Assume  $t$  is stationary,  $\delta t = 0$ .

Integrate Euler-Lagrange equations along the light path to get

deflection angle 
$$\hat{\alpha} = -\frac{2}{c^2} \int_S^O \nabla_{\perp} \phi dl$$

## Exercise: Derive the deflection angle for a point mass. I

Derive  $\hat{\alpha} = 4GM/(c^2\xi)$ .

We can approximate the potential as

$$\phi = -\frac{GM}{R} = -\frac{c^2}{2} \frac{R_S}{R},$$

where  $G$  is Newton's constant,  $M$  the mass of the object,  $R$  the distance, and  $R_S$  the Schwarzschild radius

The distance  $R$  can be written as

$$R^2 = x^2 + y^2 + z^2.$$

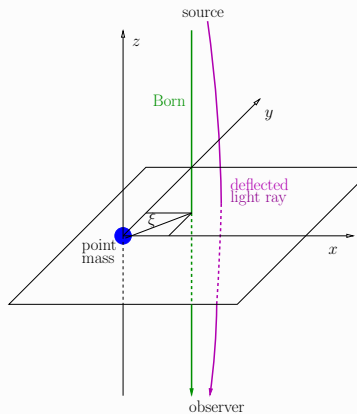
(Weak-field condition  $\phi \ll c^2$  implies  $R \gg R_S$ .)

(Here  $z$  is not redshift, but radial (comoving) distance.)

# Exercise: Derive the deflection angle for a point mass. II

We use the so-called Born approximation (from quantum mechanic scattering theory) to integrate along the unperturbed light ray, which is a straight line parallel to the  $z$ -axis with a constant  $x^2 + y^2 = \xi^2$ .

The impact parameter  $\xi$  is the distance of the light ray to the point mass.



## Exercise: Derive the deflection angle for a point mass.

### III

The deflection angle is then

$$\hat{\alpha} = -\frac{2}{c^2} \int_{-\infty}^{\infty} \nabla_{\perp} \phi \, dz.$$

The perpendicular gradient of the potential is

$$\begin{aligned} \nabla_{\perp} \phi &= -\frac{c^2 R_S}{2} \begin{pmatrix} \partial/\partial x \\ \partial/\partial y \end{pmatrix} (x^2 + y^2 + z^2)^{-1/2} \\ &= \frac{c^2 R_S}{2} \frac{1}{(\xi^2 + z^2)^{3/2}} \begin{pmatrix} x \\ y \end{pmatrix} = \frac{c^2 R_S}{2} \frac{\xi}{(\xi^2 + z^2)^{3/2}} \frac{\xi}{\xi} \end{aligned}$$

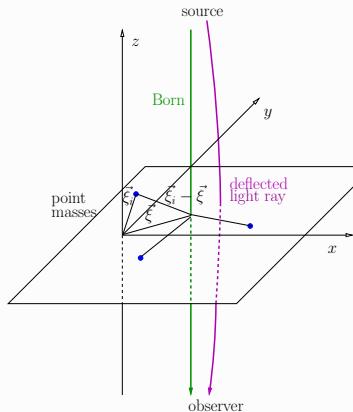
The primitive for  $(\xi^2 + z^2)^{-3/2}$  is  $z\xi^{-2}(\xi^2 + z^2)^{-1/2}$ . We get for the deflection angle

$$\hat{\alpha} = -R_S \left[ \frac{z}{\xi(\xi^2 + z^2)^{1/2}} \right]_{-\infty}^{\infty} \frac{\xi}{\xi} = -\frac{R_S}{\xi} \frac{\xi}{\xi} [1 - (-1)] = -\frac{2R_S}{\xi} \frac{\xi}{\xi} = -\frac{4GM}{c^2} \frac{\xi}{\xi^2}.$$

# Generalisation I: mass distribution I

Distribution of point masses  $M_i(\xi_i, z)$ : total deflection angle is linear vectorial sum over individual deflections.

Possible for weak fields again,  $\phi \ll c^2$ , where GR is linear.



## Generalisation I: mass distribution II

Distribution of point masses  $M_i(\boldsymbol{\xi}_i, z)$ : total deflection angle is linear vectorial sum over individual deflections

$$\hat{\alpha}(\boldsymbol{\xi}) = \sum_i \delta \hat{\alpha}(\boldsymbol{\xi} - \boldsymbol{\xi}_i) = \frac{4G}{c^2} \sum_i \delta M_i(\boldsymbol{\xi}_i, z_i) \frac{\boldsymbol{\xi} - \boldsymbol{\xi}_i}{|\boldsymbol{\xi} - \boldsymbol{\xi}_i|^2}$$

A small mass is related to a volume element via the density,  $\delta M = \rho \delta V$ .  
Perform transition to continuous density

$$\sum_i \delta M_i \rightarrow \int dM = \int \rho(\mathbf{x}) d^3x = \int d^2\xi' \int dz' \rho(\boldsymbol{\xi}', z')$$

and introduction of the 2D

$$\text{surface mass density } \Sigma(\boldsymbol{\xi}') = \int dz' \rho(\boldsymbol{\xi}', z')$$

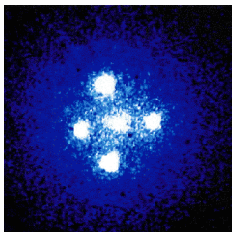
we get

$$\hat{\alpha}(\boldsymbol{\xi}) = \frac{4G}{c^2} \int d^2\xi' \Sigma(\boldsymbol{\xi}') \frac{\boldsymbol{\xi} - \boldsymbol{\xi}'}{|\boldsymbol{\xi} - \boldsymbol{\xi}'|^2}$$

**Thin-lens approximation**

# Generalisation I: mass distribution III

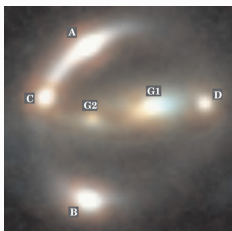
Gravitational lensing can probe complex mass profiles  $\rho$ , or (2D projected)  $\Sigma$ .



“Einstein cross”,  $z_s = 1.7$ ,  $z_l = 0.04$

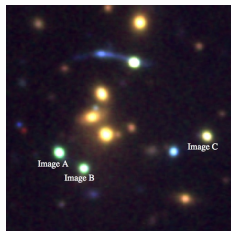


WFI2033-4723,  $z_s = 1.66$ ,  $z_l = 0.66$



CLASS B1608+656,  $z_s = 1.394$ ,  $z_l = 0.63$ .

Martin Kilbinger (CEA)

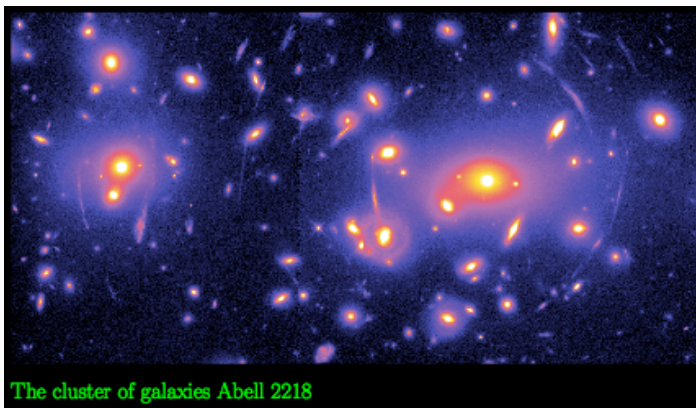


SDSS J2222+2745,  $z_s = 2.82$ ,  $z_l = 0.49$ .

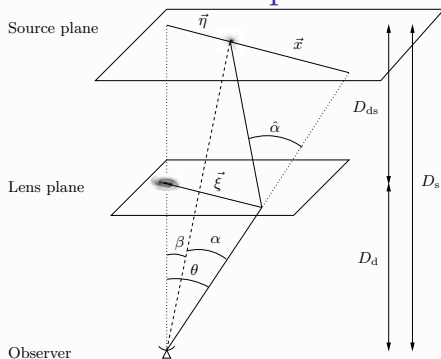
Weak lensing & Euclid

## Generalisation II: Extended source

Extended source: different light rays impact lens at different positions  $\xi$ , their deflection angle  $\alpha(\xi)$  will be different: **differential deflection**  $\rightarrow$  distortion, magnification of source image!



## Lens equation I



Intercept theorem:

$$\frac{\boldsymbol{\eta} + \boldsymbol{x}}{D_s} = \frac{\boldsymbol{\xi}}{D_d}.$$

Introducing angles

$$\beta \approx \frac{\boldsymbol{\eta}}{D_s}; \quad \theta \approx \frac{\boldsymbol{\xi}}{D_d}; \quad \hat{\alpha} = \frac{\boldsymbol{x}}{D_{ds}}$$

## Lens equation II

we find

$$\boldsymbol{\beta} + \frac{D_{\text{ds}}}{D_{\text{s}}} \hat{\boldsymbol{\alpha}} = \boldsymbol{\theta}.$$

Finally, defining the rescaled deflection angle

$$\boldsymbol{\alpha} = \frac{D_{\text{ds}}}{D_{\text{s}}} \hat{\boldsymbol{\alpha}}$$

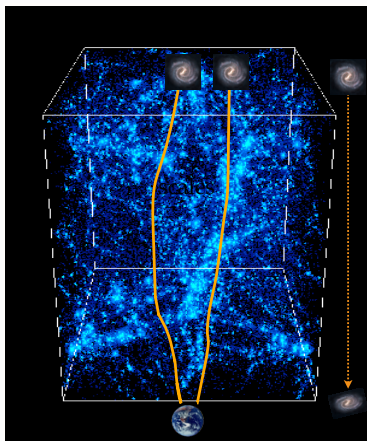
we get to

$$\boldsymbol{\beta} = \boldsymbol{\theta} - \boldsymbol{\alpha}(\boldsymbol{\theta}).$$

This simple equation relating lens to source extend is called **lens equation**

This is a mapping from lens coordinates  $\boldsymbol{\theta}$  to source coordinates  $\boldsymbol{\beta}$ . **Why?**

# Cosmic shear: continuous deflection along line of sight



With the Born approximations, and assumption that structures along line of sight are un-correlated:

Deflection angle can be written as gradient of a potential, called **lensing potential**  $\psi$ :

$$\alpha(\boldsymbol{\theta}) = \nabla\psi(\boldsymbol{\theta})$$

$$\psi(\boldsymbol{\theta}) = \frac{2}{c^2} \int_0^{\chi} d\chi' \frac{\chi - \chi'}{\chi\chi'} \Phi(\chi'\boldsymbol{\theta}, \chi').$$

for a source at comoving distance  $\chi$ .

Note: Difference between Born and actual light path up to few Mpc!

## Linearizing the lens equation

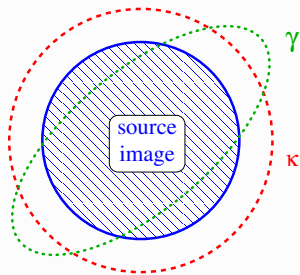
We talked about differential deflection before. To first order, this involves the derivative of the deflection angle.

$$\frac{\partial \beta_i}{\partial \theta_j} \equiv A_{ij} = \delta_{ij} - \partial_j \alpha_i = \delta_{ij} - \partial_i \partial_j \psi.$$

Jacobi (symmetric) matrix

$$A = \begin{pmatrix} 1 - \kappa - \gamma_1 & -\gamma_2 \\ -\gamma_2 & 1 - \kappa + \gamma_1 \end{pmatrix}.$$

- **convergence**  $\kappa$ : isotropic magnification
- **shear**  $\gamma$ : anisotropic stretching



Convergence and shear are second derivatives of the 2D lensing potential.

## Convergence and shear I

The effect of  $\kappa$  and  $\gamma$  follows from Liouville's theorem: Surface brightness is conserved (no photon gets lost).

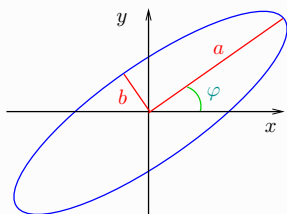
We see that **shear** transforms a circular image into an elliptical one.

Define complex shear

$$\gamma = \gamma_1 + i\gamma_2 = |\gamma|e^{2i\varphi};$$

The relation between convergence, shear, and the axis ratio of elliptical isophotes is then

$$|\gamma| = |1 - \kappa| \frac{1 - b/a}{1 + b/a}$$



## Convergence and shear II

Further consequence of lensing: **magnification**.

Liouville (surface brightness is conserved) + area changes ( $d\beta^2 \neq d\theta^2$  in general)  $\rightarrow$  flux changes.

$$\text{magnification} \quad \mu = \det A^{-1} = [(1 - \kappa)^2 - \gamma^2]^{-1}.$$

Magnification important to account for by other cosmological probes: Changes population of objects (selection effects), magnitude of standard candles (SNe Ia), standard sirens (GWs), galaxy clustering amplitude.

**Summary:** Convergence and shear linearly encompass information about projected mass distribution (lensing potential  $\psi$ ). They quantify how lensed images are magnified, enlarged, and stretched. These are the main observables in (weak) lensing.

# Convergence and cosmic density contrast

Back to the lensing potential

- Since  $\kappa = \frac{1}{2}\Delta\psi$ :

$$\kappa(\boldsymbol{\theta}, \chi) = \frac{1}{c^2} \int_0^\chi d\chi' \frac{(\chi - \chi')\chi'}{\chi} \Delta_{\boldsymbol{\theta}} \Phi(\chi' \boldsymbol{\theta}, \chi')$$

- Terms  $\Delta_{\chi'\chi'}\phi$  average out when integrating along line of sight, can be added to yield 3D Laplacian (error  $\mathcal{O}(\phi) \sim 10^{-5}$ ).
- Poisson equation

$$\Delta\Phi = \frac{3H_0^2\Omega_m}{2a} \delta \quad \left( \delta = \frac{\rho - \bar{\rho}}{\rho} \right)$$

$$\rightarrow \kappa(\boldsymbol{\theta}, \chi) = \frac{3}{2}\Omega_m \left( \frac{H_0}{c} \right)^2 \int_0^\chi d\chi' \frac{(\chi - \chi')\chi'}{\chi a(\chi')} \delta(\chi' \boldsymbol{\theta}, \chi').$$

## Convergence with source redshift distribution

So far, we looked at the convergence for one **single** source redshift (distance  $\chi$ ). Now, we calculate  $\kappa$  for a realistic survey with a redshift **distribution** of source galaxies. We integrate over the pdf  $p(\chi)d\chi = p(z)dz$ , to get

$$\kappa(\boldsymbol{\theta}) = \int_0^{\chi_{\text{lim}}} d\chi p(\chi) \kappa(\boldsymbol{\theta}, \chi) = \int_0^{\chi_{\text{lim}}} d\chi G(\chi) \chi \delta(\chi\boldsymbol{\theta}, \chi)$$

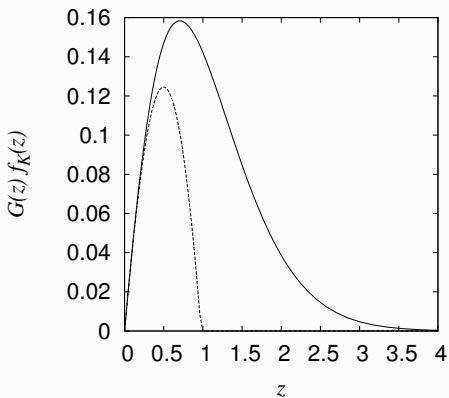
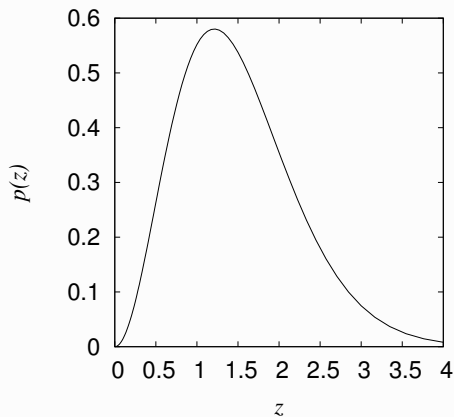
with **lens efficiency**

$$G(\chi) = \frac{3}{2} \left( \frac{H_0}{c} \right)^2 \frac{\Omega_m}{a(\chi)} \int_{\chi}^{\chi_{\text{lim}}} d\chi' p(\chi') \frac{\chi' - \chi}{\chi'}$$

The convergence is a projection of the matter-density contrast, weighted by the source galaxy distribution and angular distances.

Parametrization of redshift distribution, e.g.

$$p(z) \propto \left(\frac{z}{z_0}\right)^\alpha \exp\left[-\left(\frac{z}{z_0}\right)^\beta\right]$$



$$\alpha = 2, \beta = 1.5, z_0 = 1$$

(dashed line: all sources at redshift 1)

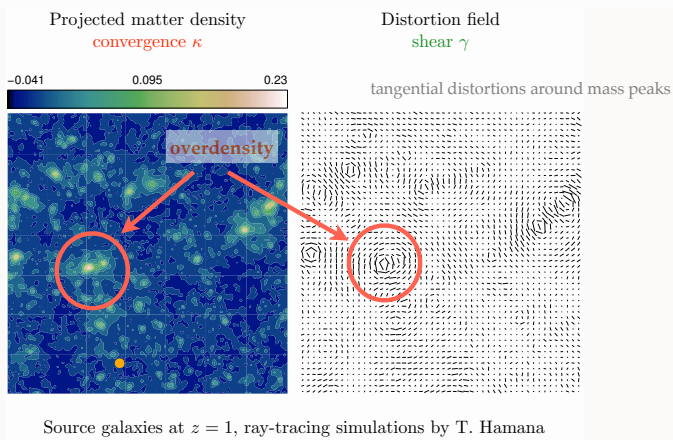
Max. lensing signal from halfway distance between us and lensing galaxies.

## More on the relation between $\kappa$ and $\gamma$

Convergence and shear are second derivatives of lensing potential  $\rightarrow$  they are related.

One can derive  $\kappa$  from  $\gamma$  (except constant *mass sheet*  $\kappa_0$ ).

E.g. get projected **mass reconstruction** of clusters from ellipticity observations.



## Basic equation of weak lensing

### Weak lensing regime

$$\kappa \ll 1, |\gamma| \ll 1.$$

The observed ellipticity of a galaxy is the sum of the intrinsic ellipticity and the shear:

$$\varepsilon^{\text{obs}} \approx \varepsilon^{\text{s}} + \gamma$$

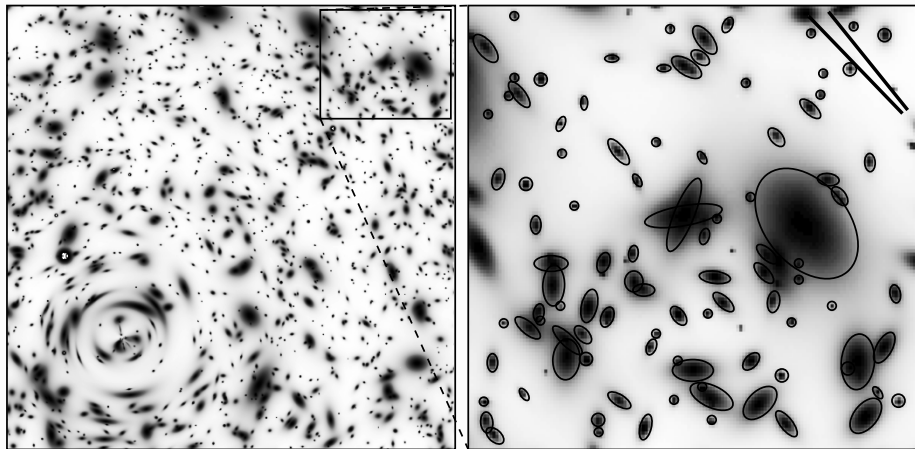
### Random intrinsic orientation of galaxies

$$\langle \varepsilon^{\text{s}} \rangle = 0 \quad \longrightarrow \quad \langle \varepsilon^{\text{obs}} \rangle = \gamma$$

The observed ellipticity is an unbiased estimator of the shear. Very noisy though!  $\sigma_\varepsilon = \langle |\varepsilon^{\text{s}}|^2 \rangle^{1/2} \approx 0.4 \gg \gamma \sim 0.03$ . Increase  $S/N$  and beat down noise by averaging over large number of galaxies.

**Question:** Why is the equivalent estimation of the convergence and/or magnification more difficult?

## Ellipticity and local shear



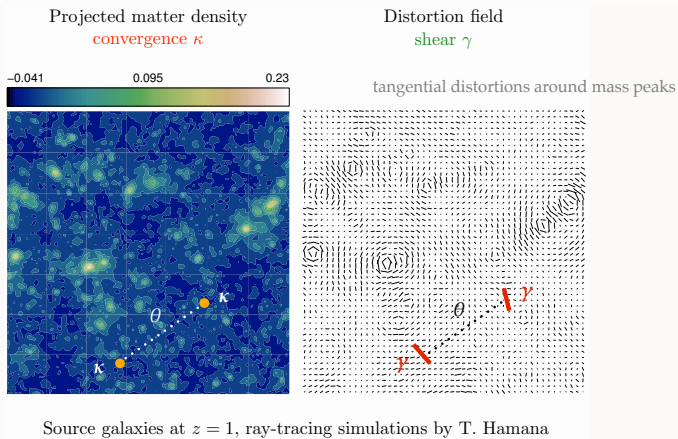
[from Y. Mellier]

Galaxy ellipticities are an estimator of the local shear.

## More on the relation between $\kappa$ and $\gamma$

Convergence and shear are second derivatives of lensing potential  $\rightarrow$  they are related.

In particular, fluctuations (variance  $\sigma^2$ ) in  $\kappa$  and  $\gamma$  are the same!



## The convergence power spectrum

- Variance of convergence  $\langle \kappa(\boldsymbol{\vartheta} + \boldsymbol{\theta})\kappa(\boldsymbol{\vartheta}) \rangle = \langle \kappa\kappa \rangle(\boldsymbol{\theta})$  depends on variance of the density contrast  $\langle \delta\delta \rangle$ .
- In Fourier space:

$$\begin{aligned}\langle \hat{\kappa}(\boldsymbol{\ell})\hat{\kappa}^*(\boldsymbol{\ell}') \rangle &= (2\pi)^2 \delta_{\text{D}}(\boldsymbol{\ell} - \boldsymbol{\ell}') P_{\kappa}(\ell) \\ \langle \hat{\delta}(\mathbf{k})\hat{\delta}^*(\mathbf{k}') \rangle &= (2\pi)^3 \delta_{\text{D}}(\mathbf{k} - \mathbf{k}') P_{\delta}(k)\end{aligned}$$

- **Limber's equation**

$$P_{\kappa}(\ell) = \int d\chi G^2(\chi) P_{\delta}\left(k = \frac{\ell}{\chi}\right)$$

using small-angle approximation,  $P_{\delta}(k) \approx P_{\delta}(k_{\perp})$ , contribution only from Fourier modes  $\perp$  to line of sight. Also assumes that power spectrum varies slowly.

- It turns out that  $P_{\kappa} = P_{\gamma}$

So we use  $\gamma$  in observations, and  $\kappa$  in modelling.

## Dependence on cosmology

**initial conditions,  
growth of structure**

$$P_{\kappa}(\ell) = \int d\chi G^2(\chi) P_{\delta} \left( k = \frac{\ell}{\chi} \right)$$

$$G(\chi) = \frac{3}{2} \left( \frac{H_0}{c} \right)^2 \frac{\Omega_m}{a(\chi)} \int_{\chi}^{\chi_{\text{lim}}} d\chi' p(\chi') \frac{\chi' - \chi}{\chi'}$$

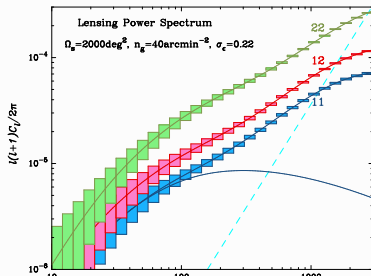
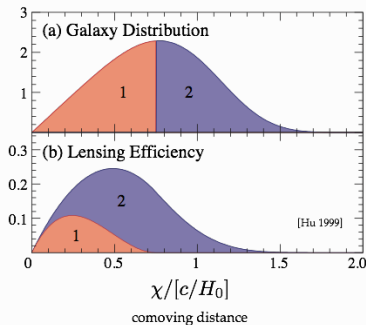
**matter density**

**redshift distribution  
of source galaxies**

**geometry**

# Lensing 'tomography' (2 1/2 D lensing)

- Bin galaxies in redshift.
- Lensing efficiency depends on bins: measure  $z$ -depending expansion and growth history.
- Necessary to measure dark energy, modified gravity.



$$P_{\kappa}(\ell) = \int_0^{\chi_{\text{lim}}} d\chi G^2(\chi) P_{\delta} \left( k = \frac{\ell}{\chi} \right) \rightarrow$$

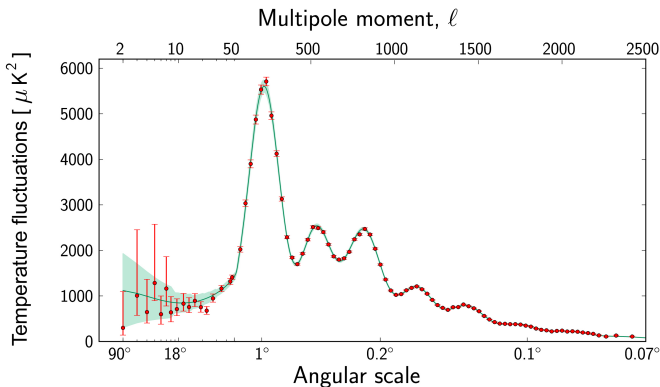
$$P_{\kappa}^{ij}(\ell) = \int_0^{\chi_{\text{lim}}} d\chi G_i(\chi) G_j(\chi) P_{\delta} \left( k = \frac{\ell}{\chi} \right)$$

$$G_i(\chi) = \frac{3}{2} \left( \frac{H_0}{c} \right)^2 \frac{\Omega_m}{a(\chi)} \int_{\chi}^{\chi_{\text{lim}}} d\chi' p_i(\chi') \frac{\chi' - \chi}{\chi'}$$

Question: Why does  $P_{\kappa}$  increase with  $z$ ?

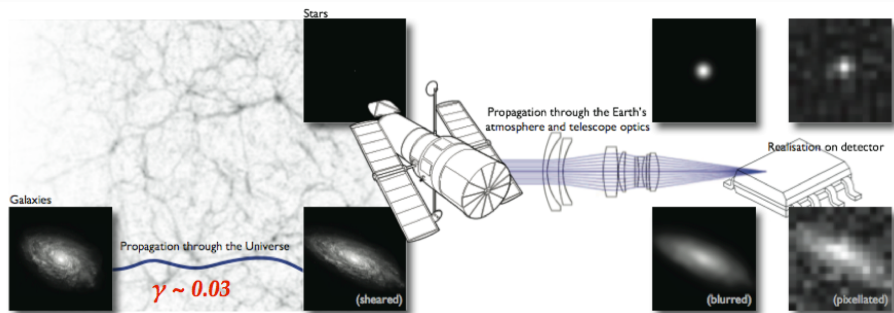
## Comparison to CMB angular power spectrum

Unlike CMB  $C_\ell$ 's, features in matter power spectrum are washed out by projection and non-linear evolution.



[Planck Consortium]

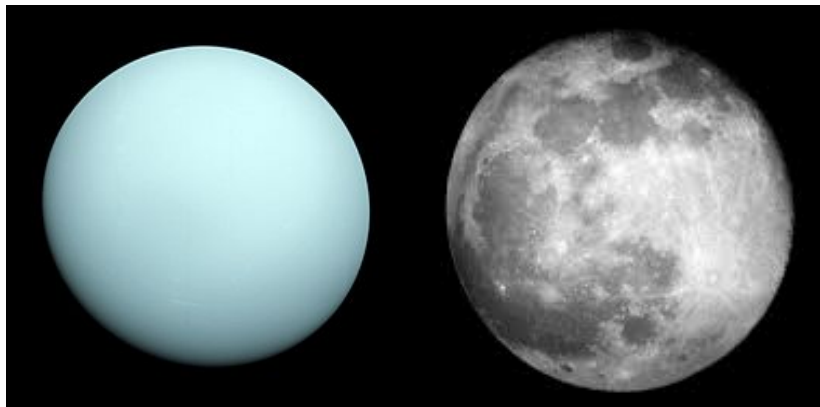
# The shape measurement challenge



Bridle et al. 2008, great08 handbook

- Cosmological shear  $\gamma \ll \epsilon$  intrinsic ellipticity
- Galaxy images corrupted by PSF (point-spread function)
- Measured shapes are biased

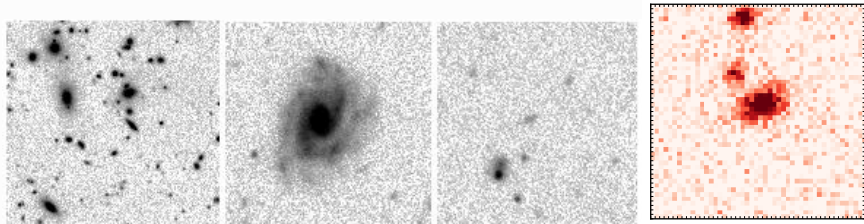
## Measuring cosmic shear



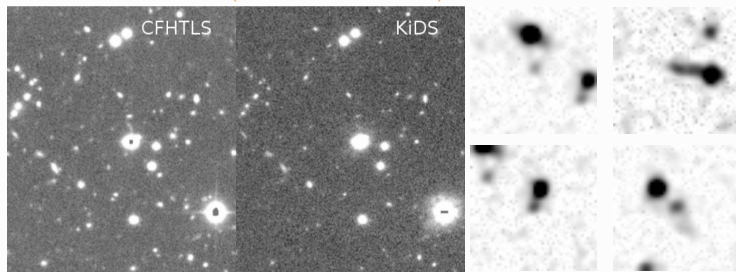
Typical shear of a few percent equivalent to difference in ellipticity between Uranus and the Moon.

# The shape measurement challenge

How do we measure “ellipticity” for irregular, faint, noisy objects?



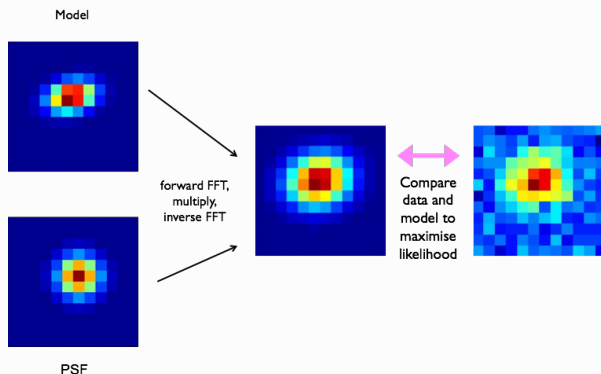
[Y. Mellier/CFHT(?)] — (Jarvis et al. 2016)



[CFHTLenS/KiDS image — CFHTLenS postage stamps]

# Shape measurement

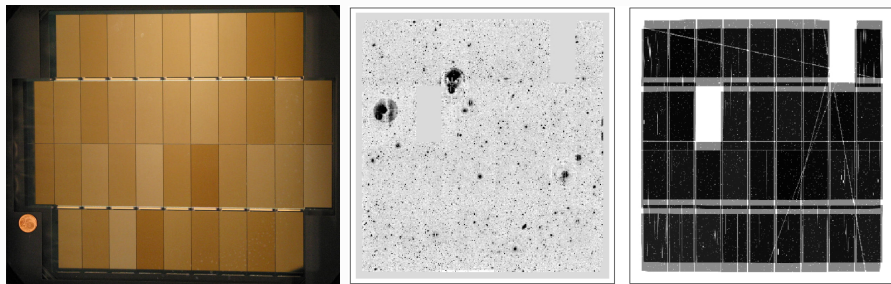
## Example: Model fitting



## Forward model-fitting (example *lensfit*)

- Convolution of model with PSF instead of deconvolution of image
- Combine multiple exposures (in Bayesian way, multiply posterior density), avoiding co-adding of (dithered) images

# Dithering



Left: Image of the MegaCam focal plane (CCD array). (4 new chips were added recently.)

Middle: Co-add of two  $r$ -band exposures of CFHTLenS (without the 4 new CCDs).

Right: Weight map.

# Shear measurement biases I

## Origins

- **Noise bias:** In general, ellipticity is non-linear in pixel data (e.g. normalization by flux). Pixel noise  $\rightarrow$  biased estimators.
- **Model bias:** Assumption about galaxy light distribution is in general wrong.
- **Other:** Imperfect PSF correction, detector effects (CTI — charge transfer inefficiency), selection effects (probab. of detection/successful  $\varepsilon$  measurement depends on  $\varepsilon$  and PSF)

## Characterisation

Bias can be multiplicative ( $m$ ) and additive ( $c$ ):

$$\gamma_i^{\text{obs}} = (1 + m)\gamma_i^{\text{true}} + c; \quad i = 1, 2.$$

Biases  $m, c$  are typically complicated functions of galaxy properties (e.g. size, magnitude, ellipticity), redshift, PSF, .... They can be scale-dependent.

Current methods:  $|m| = 1\% - 10\%$ ,  $|c| = 10^{-3} - 10^{-2}$ .

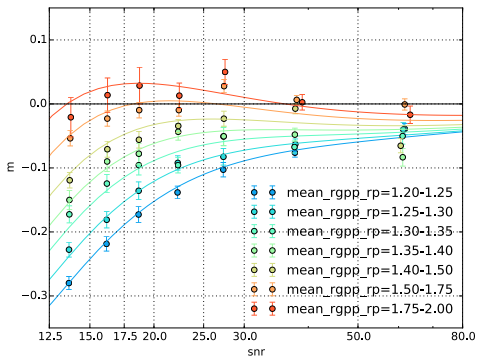
Blind simulation challenges have been run to quantify biases, getting ideas from computer science community (e.g. <http://great3challenge.info>).

# Shear measurement biases II

## Calibration

Using simulated or emulated data (or self-calibration).

Functional dependence of  $m$  on observables must not be too complicated (e.g. not smooth, many variables, large parameter space), or else measurement is *not calibratable!*



(Jarvis et al. 2016) - image simulations

## Requirements for surveys

Necessary knowledge of residual biases  $|\Delta m|, |\Delta c|$  (after calibration):

Current surveys 1%.

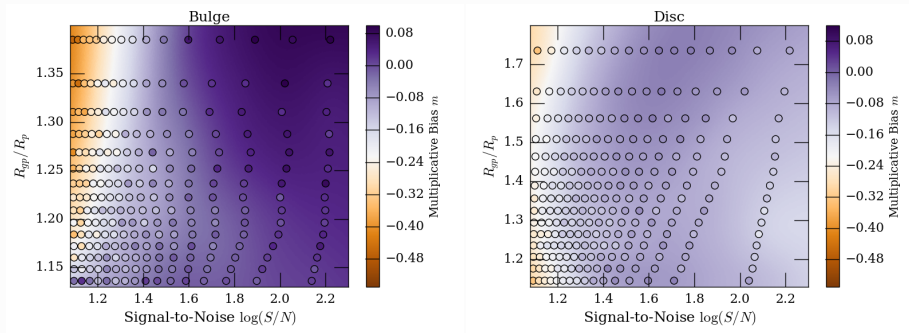
Future large missions (Euclid, LSST, ...)  $10^{-4} = 0.1\%$ !

# Shear measurement biases III

## Complex bias dependencies

Need to account for bias as function of more than one galaxy property.

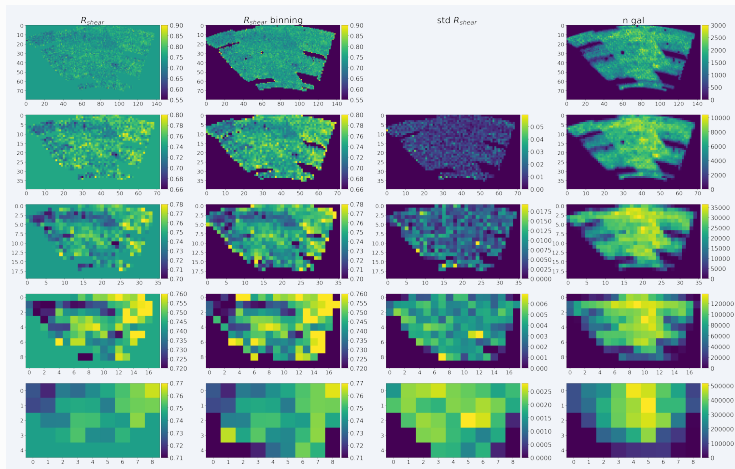
E.g. size and SNR. Also need to know bulge and disc fraction of observed population.



(Zuntz et al. 2018)

## Shear measurement biases IV

## Local bias measurement

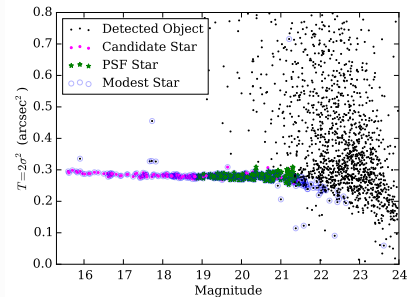


[CFIS patch P3]

(Ayçoberry et al. 2022)

[M2 stage 2021.]

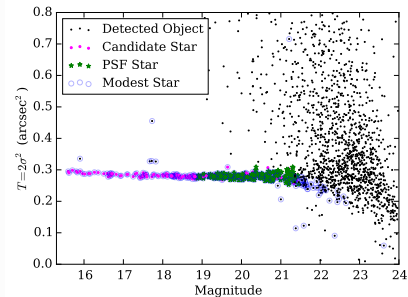
## PSF correction



(Jarvis et al. 2016)

- Select clean sample of stars
- Measure star shapes
- Create PSF model and interpolate (pixel values, ellipticity, PCA coefficients, ...) to galaxy positions. Space-based observations: global PSF model from many exposures possible
- Correct for PSF: galaxy image deconvolution or other (e.g. linearized) correction, or convolve model

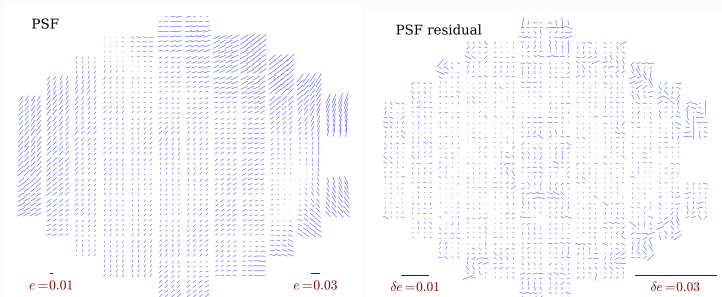
## PSF correction



(Jarvis et al. 2016)

- Select clean sample of stars
- Measure star shapes
- Create PSF model and interpolate (pixel values, ellipticity, PCA coefficients, ...) to galaxy positions. Space-based observations: global PSF model from many exposures possible
- Correct for PSF: galaxy image deconvolution or other (e.g. linearized) correction, or convolve model

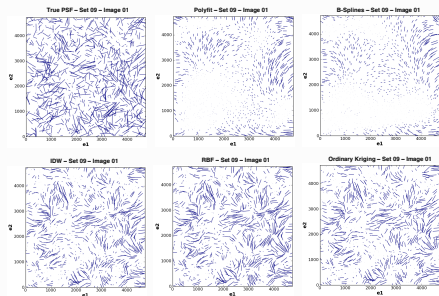
# PSF correction



(Jarvis et al. 2016)

- Select clean sample of stars
- Measure star shapes
- Create PSF model and interpolate (pixel values, ellipticity, PCA coefficients, ...) to galaxy positions. Space-based observations: global PSF model from many exposures possible
- Correct for PSF: galaxy image deconvolution or other (e.g. linearized) correction, or convolve model

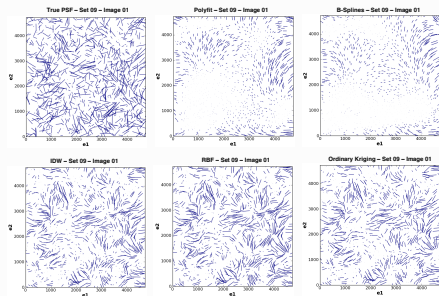
# PSF correction



(Gentile et al. 2013)

- Select clean sample of stars
- Measure star shapes
- Create PSF model and interpolate (pixel values, ellipticity, PCA coefficients, ...) to galaxy positions. Space-based observations: global PSF model from many exposures possible
- Correct for PSF: galaxy image deconvolution or other (e.g. linearized) correction, or convolve model

# PSF correction

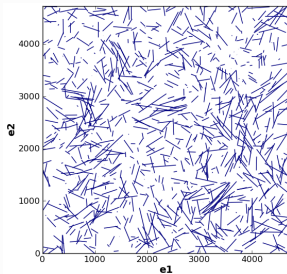


(Gentile et al. 2013)

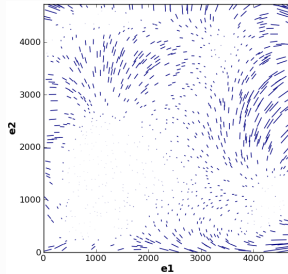
- Select clean sample of stars
- Measure star shapes
- Create PSF model and interpolate (pixel values, ellipticity, PCA coefficients, ...) to galaxy positions. Space-based observations: global PSF model from many exposures possible
- Correct for PSF: galaxy image deconvolution or other (e.g. linearized) correction, or convolve model

## PSF interpolation

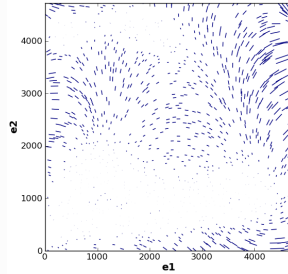
True PSF – Set 09 – Image 01



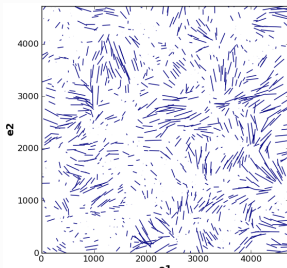
Polyfit – Set 09 – Image 01



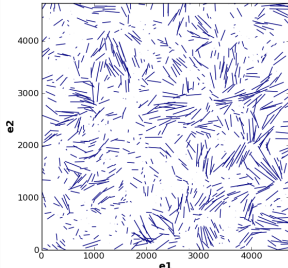
B-Splines – Set 09 – Image 01



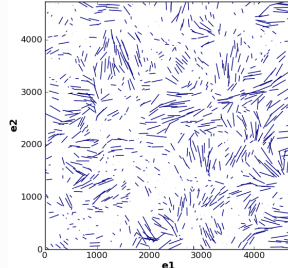
IDW – Set 09 – Image 01



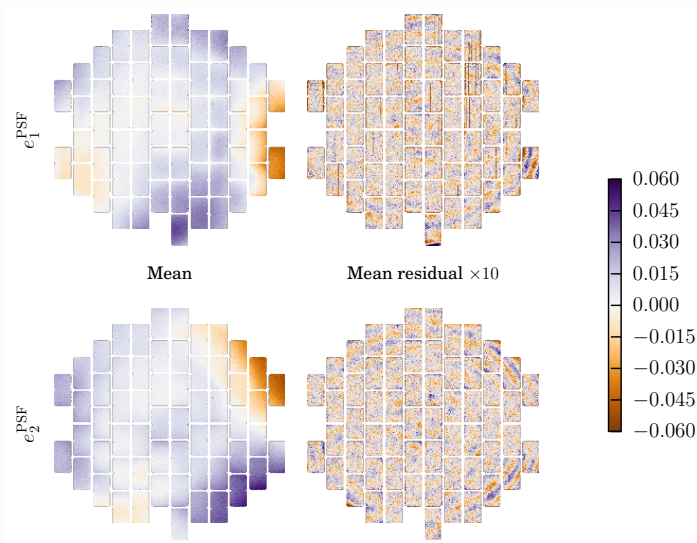
RBF – Set 09 – Image 01



Ordinary Kriging – Set 09 – Image 01

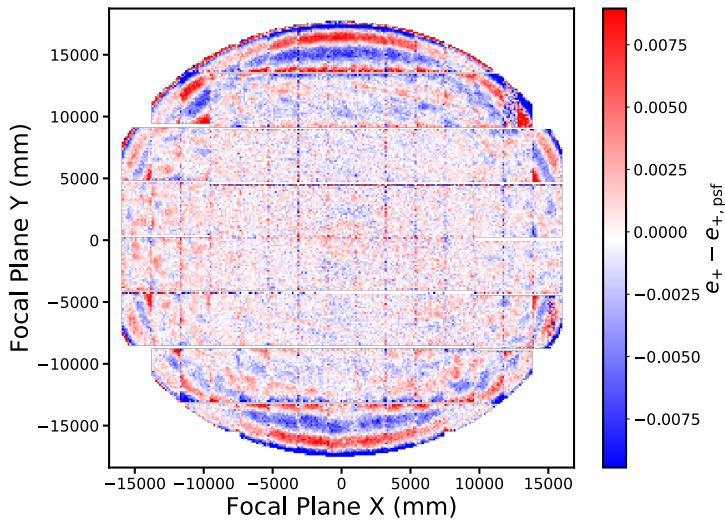


## PSF model residuals, more examples



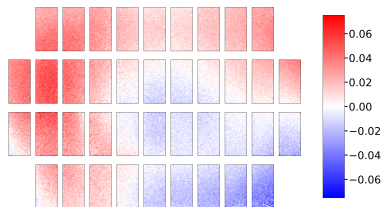
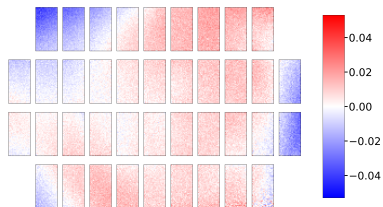
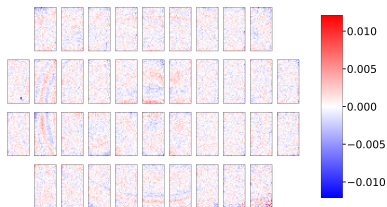
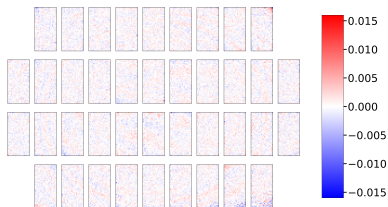
DES-Y1, (Zuntz et al. 2018)

## PSF model residuals, more examples



HSC, (Mandelbaum 2018)

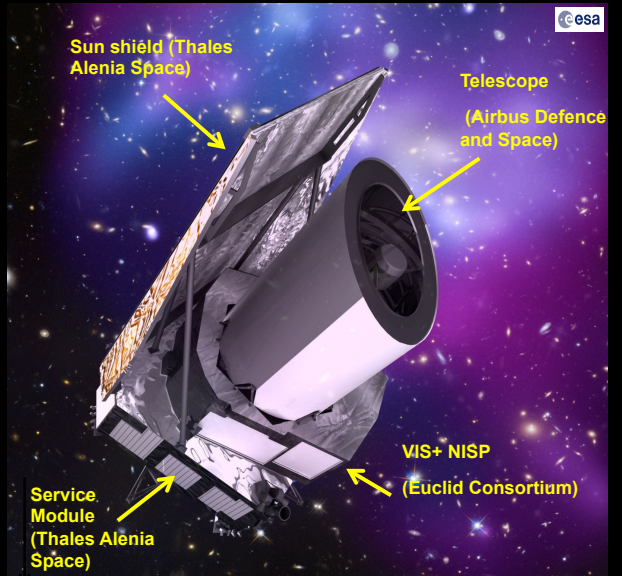
## PSF model residuals, more examples

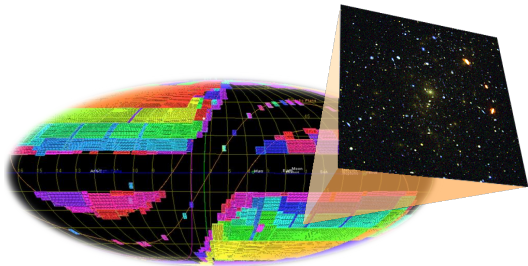
 $e_1$  model $e_2$  model $e_1$  residuals $e_2$  residuals

CFIS, (Guinot et al. 2022)

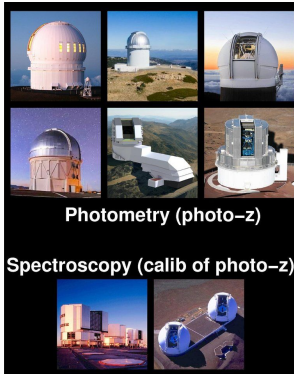
# ESA Euclid mission:

- Total mass satellite :  
2 200 kg
- Dimensions:  
4,5 m x 3 m
- **Launch:** end 2020 by a Soyuz rocket from the Kourou space port  
Euclid placed in L2
- **Survey:** 6 years,





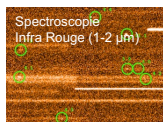
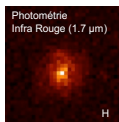
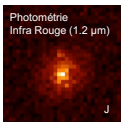
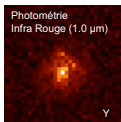
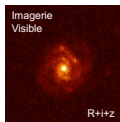
Euclid area = 15,000 deg<sup>2</sup> (extra-galactic and -ecliptic sky).



Photometry (photo-z)

Spectroscopy (calib of photo-z)

Ground-based observations for photometric redshifts.



**10 billions of galaxies observed in visible and infra red photometry**

**50 millions of infra red spectra**

Euclid imaging and spectroscopy.

# Euclid

## Two instruments:

- Visible imager, WL,  $1.5 \times 10^9$  galaxies
- Near-IR imager + spectrograph,  $3 \times 10^7$  galaxy spectra

## Cosmology

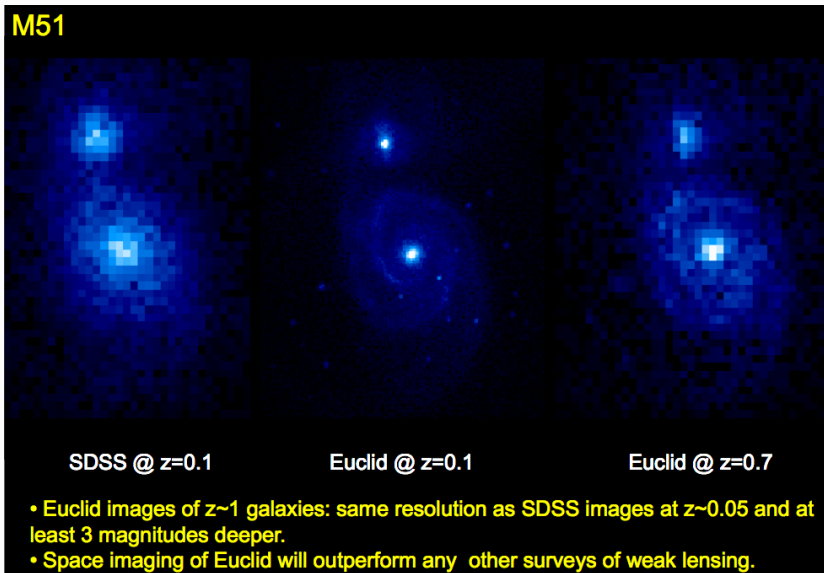
- Dark-energy equation of state  $w$  to 2% (currently  $\sim 20\%$ )
- Constrain models of modified gravity
- Neutrino masses to 0.02 eV (currently  $\sim 0.3$  eV)
- Map dark matter distribution
- Early-universe conditions, inflation: limit non-Gaussianity  $f_{\text{NL}}$  to  $\pm 2$  (currently  $\sim \pm 6$ )

## “Legacy”

- High-redshift galaxies, AGN & clusters @  $z > 1$ , QSO @  $z > 8$ , strong lensing galaxy candidates: Increase of numbers by several orders of magnitude

## Euclid imaging

M51

SDSS @  $z=0.1$ Euclid @  $z=0.1$ Euclid @  $z=0.7$ 

- Euclid images of  $z\sim 1$  galaxies: same resolution as SDSS images at  $z\sim 0.05$  and at least 3 magnitudes deeper.
- Space imaging of Euclid will outperform any other surveys of weak lensing.

# Euclid WL challenge: PSF

PSF is complex, diffraction-limited.

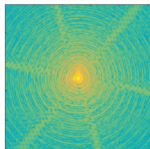
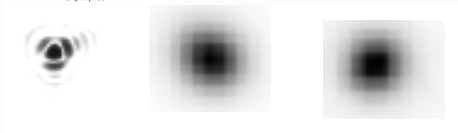
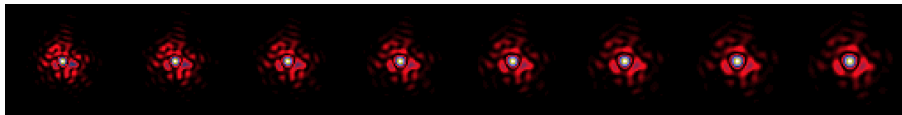


Figure 5-2 - VIS channel system PSF realization (log display)

PSF is undersampled.



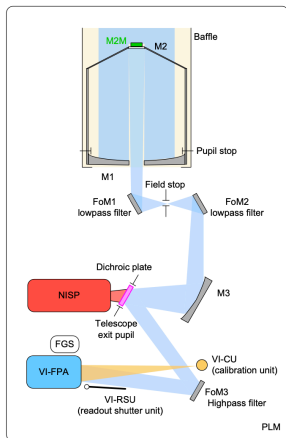
PSF varies with wavelength over broad VIS band.



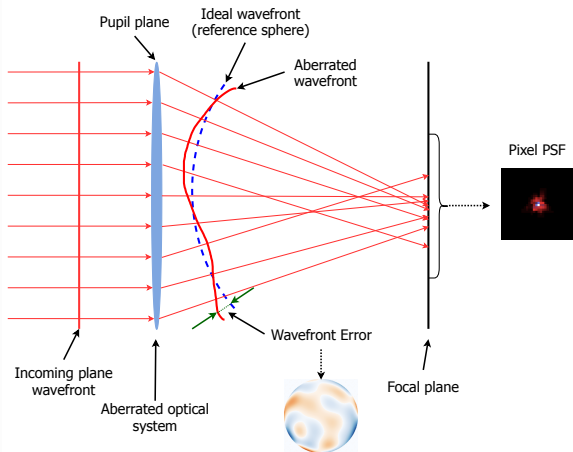
(Liaudat et al. 2022)

# Euclid WL challenge: PSF

Modelling PSF in wavefront instead of pixel space.



(a)

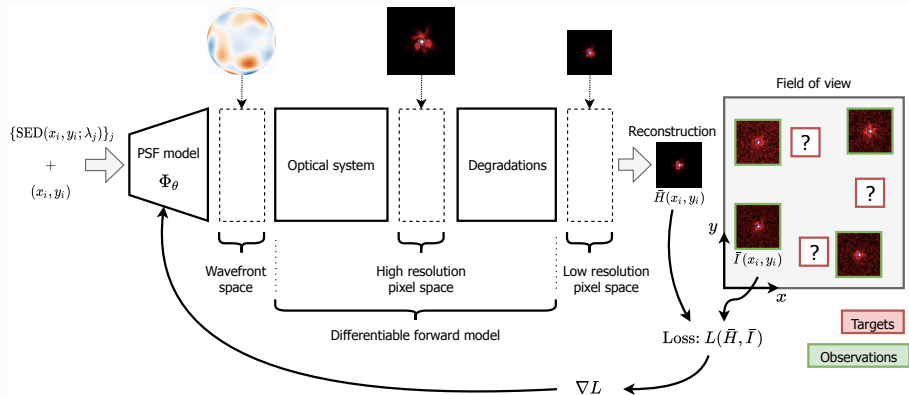


(b)

(Liaudat et al. 2022)

## Euclid WL challenge: PSF

Differentiable forward-model.



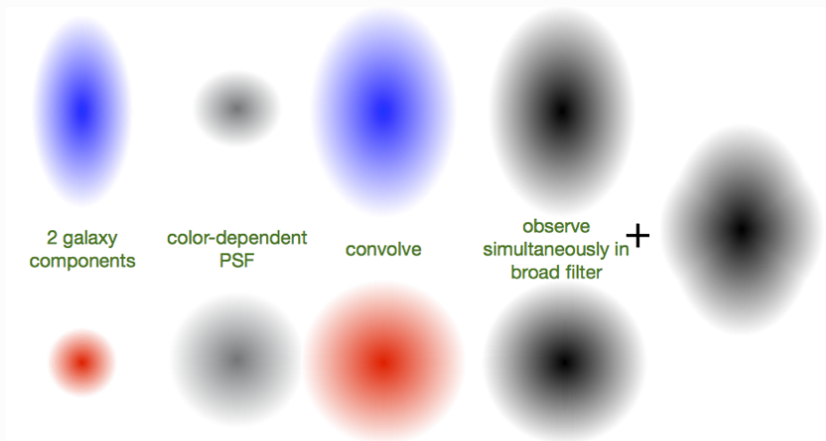
(Liaudat et al. 2022)

# Further PSF modelling: JWST



## Euclid WL challenges

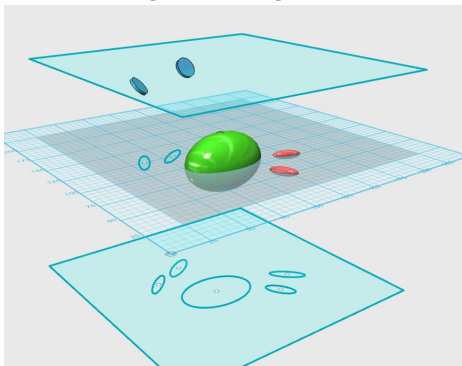
## Color gradients



Euclid observes without optical filter (equiv.  $R + I + z$ ). Calibrate color effects using HST multi-band observations.

# Euclid WL challenges

## Intrinsic alignment of galaxies



Galaxy shapes are correlated to surrounding tidal density field. Shape of galaxies is sum of shear ( $G$ ) and intrinsic ( $I$ ) shape (remember  $\varepsilon \approx \varepsilon^s + \gamma$ ).

The total correlation of galaxy shapes is not only shear-shear ( $GG$ ), but also intrinsic-intrinsic ( $II$ ) and shear-intrinsic ( $GI$ ; (Hirata & Seljak 2004)).

(Joachimi et al. 2015)

Contamination to cosmic shear at  $\sim 1 - 10\%$ .

Need to model galaxy formation.

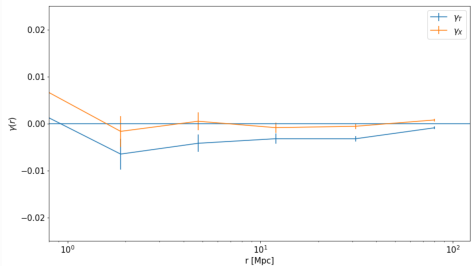
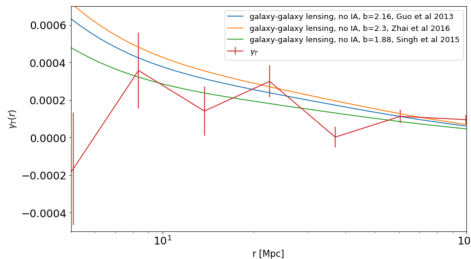
Not well known, in particular at high  $z$  and low halo masses.

# Intrinsic alignment measurements

Measurement of galaxy-galaxy lensing (bg - fg galaxy pairs) and intrinsic alignments (fg - fg galaxy pairs) in CFIS survey.

Learn about:

- IA as function of galaxy type, redshift, environment.
- Galaxy formation and evolution in dark-matter halos.
- Bias and mitigation strategies for Euclid cosmology.



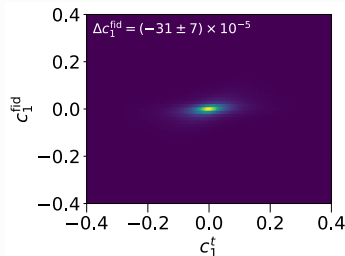
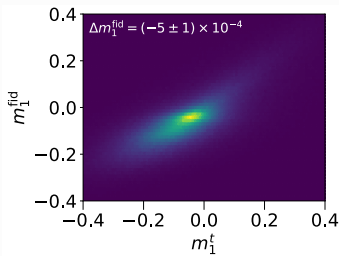
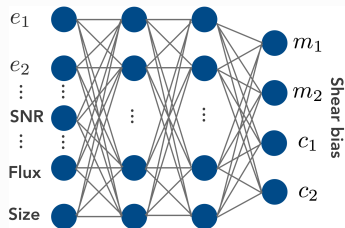
[Elisa Russier, M2 stage 2022.]

# Shear calibration from deep learning I

Train neural network to learn (via linear regression) shear bias as function of observed galaxy (and PSF) properties.

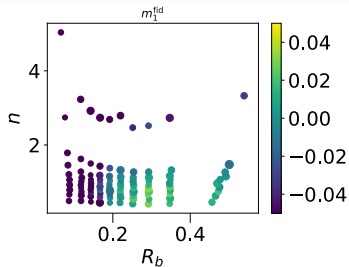
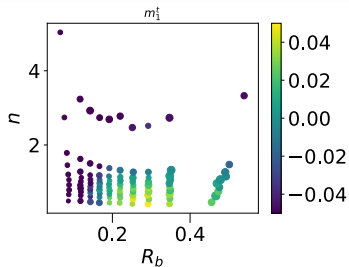
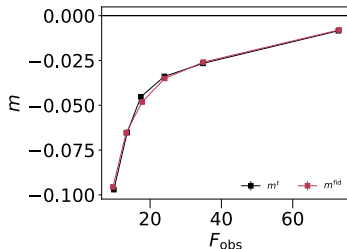
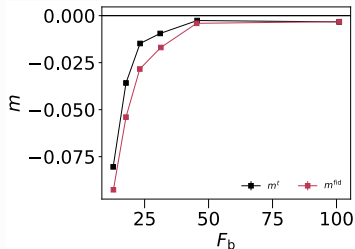
NN automatically finds most relevant input quantities to predict shear bias.

Using trained network (model), use real data as input to estimate shear bias.



(Pujol et al. 2020)

## Shear calibration from deep learning II



(Pujol et al. 2020)

# Metacalibration

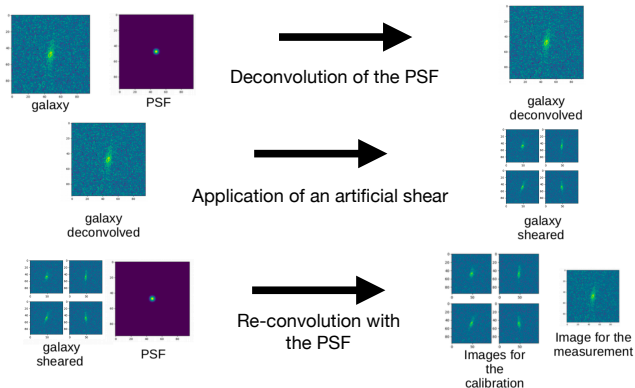
Reminder: Shear bias.

$$\gamma_i^{\text{obs}} = (1 + m)\gamma_i^{\text{true}} + c; \quad i = 1, 2.$$

Multiplicative bias  $m$  can be interpreted as response of observed to true shear.

$$m = \partial\gamma_i^{\text{obs}} / \gamma_i^{\text{true}}.$$

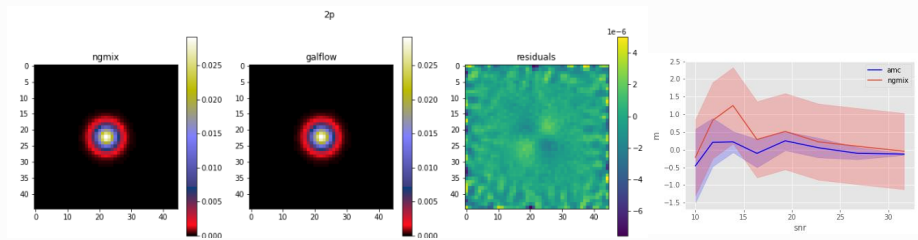
Estimate by applying artificial shear to galaxy images, finite differences.



# Metacalibration+: automatic differentiation

Further development of metacalibration (1/2): *galflow*, *autocal*

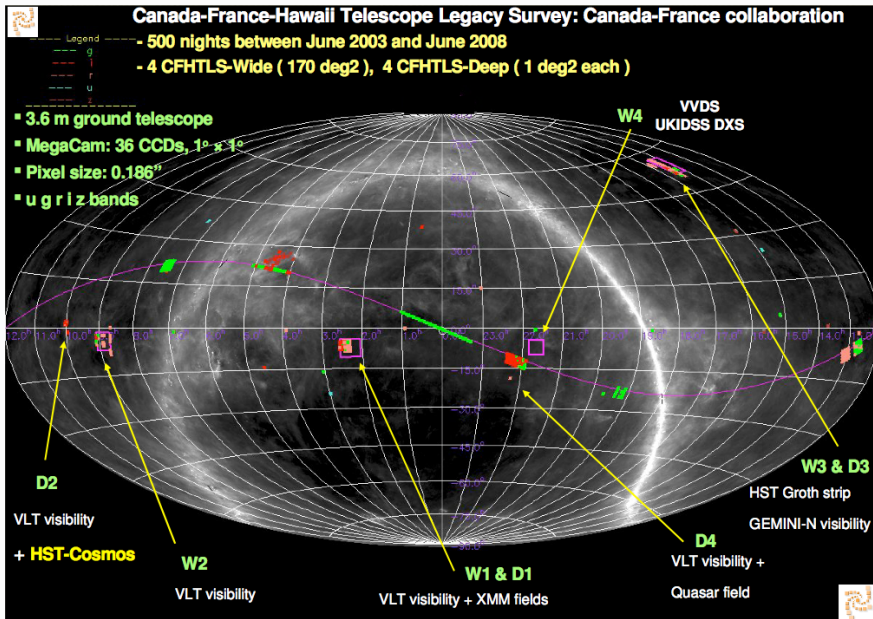
- Use *automatic differentiation* to replace finite differences.
- (Re-)implement metacalibration in `tensorflow`.
- All differentiable operations (pixellisation, shearing, convolution, ...), are “recorded”, gradients can be computed automatically, without the need of numerical derivatives.
- No need to generate 4 additional images
- Hope: Reconvolution PSF smaller, better noise properties



[Figure from André Zamorano Vitorelli.]

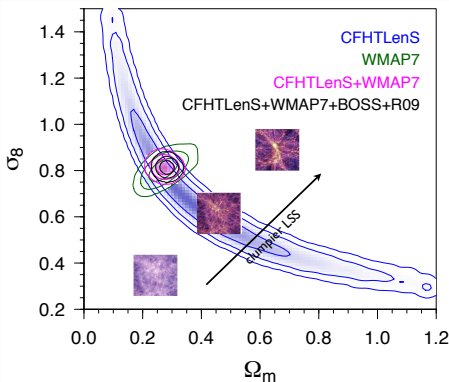
# Results from weak-lensing surveys

1. Early era: 2000 - 2006
2. Consolidating era: 2007 – 2012
3. Small-survey era: 2013 – 2016
4. Medium survey era: 2017 – 2021
5. Large survey era: 2022 – 2030

State of the art  $\sim 2013$ : CFHTLenS

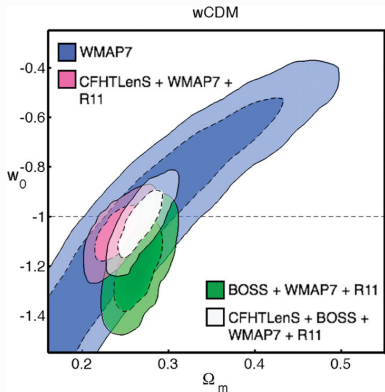
State of the art  $\sim 2013$ 

## CFHTLenS



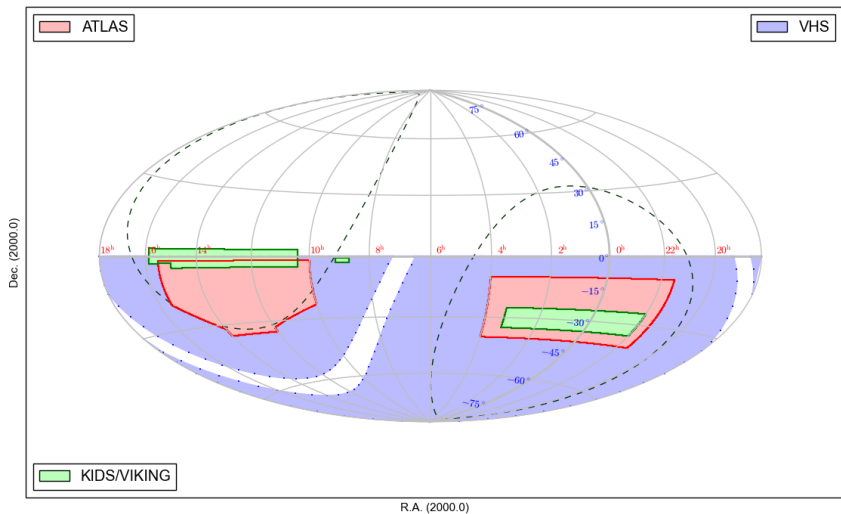
2D lensing  
(Kilbinger et al. 2013)

( $\sigma_8$ : power-spectrum normalisation; RMS of density fluct. in 8 Mpc spheres.)

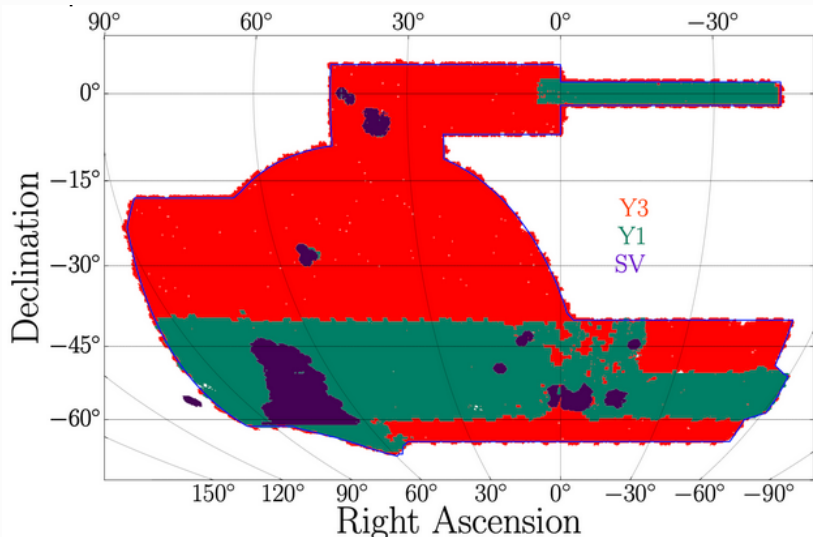


6-bin tomography  
(Heymans et al. 2013)

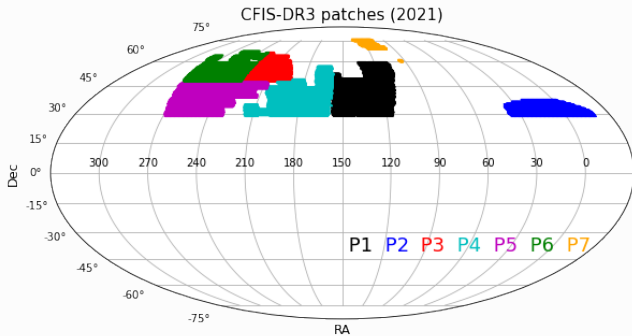
## Ongoing surveys: KiDS



## Ongoing surveys: DES



## Ongoing surveys: UNIONS/CFIS

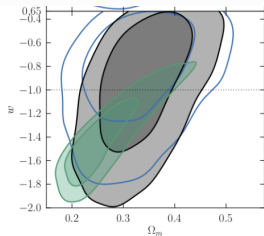
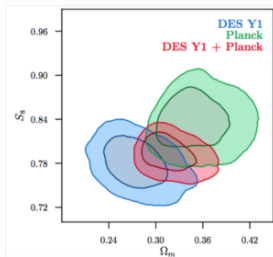


CFHT:  $u, r$ . Pan-STARRS:  $i, z$ . Subaru-HSC:  $g, z$ .

Part of Euclid survey to provide photometric redshifts in Northern sky.

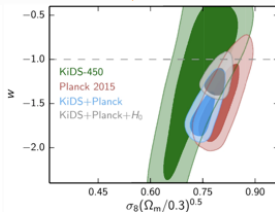
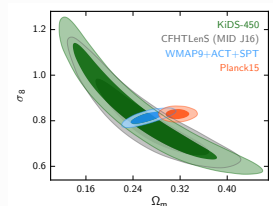
3,500/5,000  $\text{deg}^2$  analysed, 100 million weak-lensing galaxies.

Excellent image quality (median seeing  $\sim 0.65''$ ). Overlap with deep spectroscopic data from SDSS+eBOSS, DESI.

Some more results  $\sim$  2017

(DES Coll. et al. 2017) - DES WL + GC

(Troxel et al. 2017) - DES



(Hildebrandt et al. 2017) - KiDS

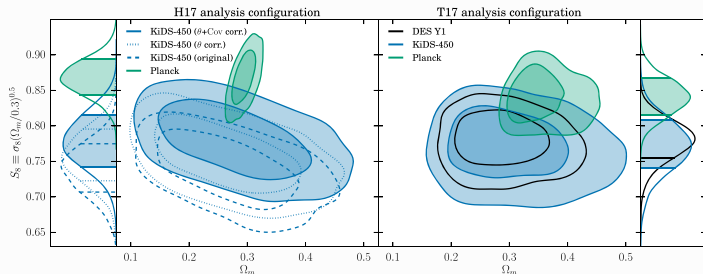
(Joudaki et al. 2017) - KiDS

# Discrepancy with Planck? I

- Only 2 - 3 $\sigma$ . However, also discrepancy of CMB  $C_\ell$ 's with SZ cluster counts.
- Additional physics, e.g. massive neutrinos? Not sufficient evidence.
- WL systematics? (E.g. shear bias, baryonic uncertainty on small scales.) KiDS say not likely.

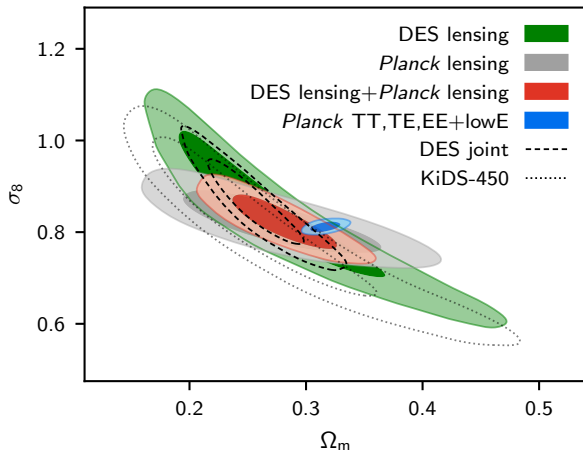
## Updates

1. Weak-lensing, (Troxel et al. 2018). Improved computation of shape noise, shear bias correction, and angular scales weighting.



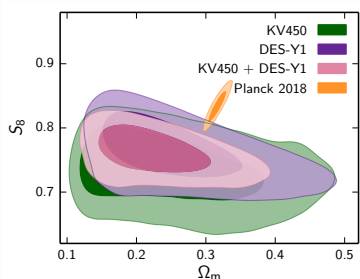
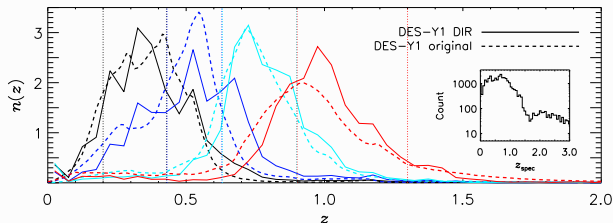
## Discrepancy with Planck? II

## 2. Planck 2018 results, (Planck Collaboration et al. 2018)



## Discrepancy with Planck? III

## 3. KiDS + DES, redshift calibration.



(Joudaki et al. 2019)

## Bibliography I

-  Açoberry E, Ajani V, Guinot A, Kilbinger M, Pettorino V & al. 2022 *arXiv e-prints* p. arXiv:2204.06280.
-  DES Coll., Abbott T M C, Abdalla F B, Alarcon A, Aleksić J & al. 2017 *arXiv* **1708.01530**.
-  Einstein A 1915 *Sitzungsberichte der Königlich Preußischen Akademie der Wissenschaften (Berlin)*, Seite 844-847. .
-  Gentile M, Courbin F & Meylan G 2013 *A&A* **549**, A1.
-  Guinot A, Kilbinger M, Farrens S, Peel A, Pujol A & al. 2022 *arXiv e-prints* p. arXiv:2204.04798.
-  Heymans C, Grocutt E, Heavens A, Kilbinger M, Kitching T D & al. 2013 *MNRAS* **432**, 2433–2453.
-  Heidebrandt H, Viola M, Heymans C, Joudaki S, Kuijken K & al. 2017 *MNRAS* **465**, 1454–1498.
-  Hirata C M & Seljak U 2004 *Phys. Rev. D* **70**(6), 063526–+.
-  Jarvis M, Sheldon E, Zuntz J, Kacprzak T, Bridle S L & al. 2016 *MNRAS* **460**, 2245–2281.

## Bibliography II

-  Joachimi B, Cacciato M, Kitching T D, Leonard A, Mandelbaum R & al. 2015 *Space Sci. Rev.* **193**, 1–65.
-  Joudaki S, Hildebrandt H, Traykova D, Chisari N E, Heymans C & al. 2019 *arXiv e-prints* p. arXiv:1906.09262.
-  Joudaki S, Mead A, Blake C, Choi A, de Jong J & al. 2017 *MNRAS* **471**, 1259–1279.
-  Kilbinger M, Fu L, Heymans C, Simpson F, Benjamin J & al. 2013 *MNRAS* **430**, 2200–2220.
-  Laudat T, Starck J L, Kilbinger M & Frugier P A 2022 *arXiv e-prints* p. arXiv:2203.04908.
-  Mandelbaum R 2018 *ARA&A* **56**, 393–433.
-  Planck Collaboration, Aghanim N, Akrami Y, Ashdown M, Aumont J & al. 2018 *ArXiv e-prints* .
-  Potter D, Stadel J & Teyssier R 2016 *ArXiv e-prints* .
-  Pujol A, Bobin J, Sureau F, Guinot A & Kilbinger M 2020 *A&A* **643**, A158.

## Bibliography III

-  Springel V, White S D M, Jenkins A, Frenk C S, Yoshida N & al. 2005 *Nature* **435**, 629–636.
-  Troxel M A, Krause E, Chang C, Eifler T F, Friedrich O & al. 2018 *MNRAS* **479**, 4998–5004.
-  Troxel M A, MacCrann N, Zuntz J, Eifler T F, Krause E & al. 2017 *arXiv* **1708.01538**.
-  Walsh D, Carswell R F & Weymann R J 1979 *Nature* **279**, 381–384.
-  Zuntz J, Sheldon E, Samuroff S, Troxel M A, Jarvis M & al. 2018 *MNRAS* **481**, 1149–1182.